# Numerical Simulation of the Platinum $L_{III}$ Edge White Line Relative to Nanometer Scale Clusters

**D. Bazin,*,† D. Sayers,‡ J. J. Rehr,§ and C. Mottet||**

*LURE, Bât. 209 D, Université Paris-Sud, 91405 Orsay Cedex, France, Department of Physics, North Carolina State University, Raleigh, North Carolina 27695-8202, Department of Physics, Washington University, Seattle, Washington 98195, and CRMC², Campus de luminy, Case 913, 13288, Marseille Cedex 9, France*

*Received: December 2, 1996; In Final Form: May 2, 1997*[⊗]

From an experimental point of view and more particularly in heterogeneous catalysis, the $L_{III}$ white line is at the center of electronic charge transfer either between either the nanometer scale metallic particle and the support or between the two metals which are present inside the cluster. In this work, we show that a strong correlation exists between the intensity of the white line and the size of the cluster. Thus, at least two physical phenomenon can affect the intensity of the white line: the size of the cluster, which can be considered as an intrinsic effect (density of state of nanometer scale platinum cluster are far from the bulk one), and a possible charge transfer between the cluster and the support, which can be considered as an extrinsic one. If the first results obtained with the FeFF program are encouraging, it is clear that to go further in the analysis, the detailed geometric configurations present in the cluster surface have to be integrated very precisely in order to obtain quantitative effects that would be more clearly related to the characteristics of the density of states.

## 1. Introduction

At the $L_{III}$ X-ray absorption edge (XANES), a phenomenon discovered a long time ago[1] and called the "white line" is often observed. It is interpreted as due to electronic transitions from a core level, $2p_{3/2}$ for the $L_{III}$ edge, to vacant d states of the absorbing atom and is thus distinct from the extended X-ray absorption fine structure.[2−9] Quickly recognized as a powerful tool to characterize *in situ* d-electron configuration in catalysts,[10,11] it has motivated numerous works performed on monometallic or multimetallic systems to determine charge transfer between either the metallic particle and the support or the molecule adsorbed at the surface of the particle,[12−14] or between the two metals present inside the particle.[15,16] Because this approach can be made *in situ*,[17] experiments are made either after[18] or during the chemical reaction.[19,20]

In this work, we consider nanometer scale sized metallic clusters which are classically used in numerous industrial processes such as reforming or postcombustion. For this kind of material, we try to define an experimental approach using the different techniques related to synchrotron radiation. In particular the necessity to use X-ray absorption spectroscopy as well as anomalous diffraction in order to obtain a fine structural description has already been underlined.[21−27] Moreover, using new codes liked FEFF based on the development of the scattering series[28−30] or CONTINUUM,[31] it has been shown that the XANES of K absorption edge can be used to obtain information regarding the size of the metallic particle.[32,33]

Let us now consider the $L_{III}$ edge and more particularly the so-called "white line" to evaluate the effect of different parameter on this particular feature. We will focus here on nanometer scale platinum clusters with the FCC structure ($O_h$ symmetry), namely, cuboctahedra with 13 and 55 atoms.

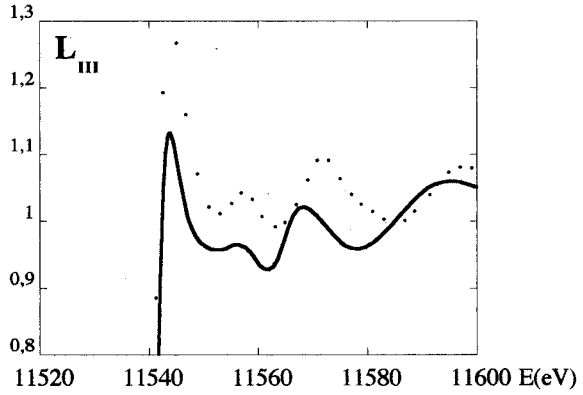


**Figure 1.** Comparison between the white line associated with the platinum foil calculated with FeFF6 (dots) and experimental (line).

## 2. Comparison between FEFF6 and FEFF7

Numerous works deal with the simulation of the XANES spectrum of the platinum metallic foil that exhibits the so-called white line. As pointed by Zabinsky et al.,[34,35] this edge is generally reproduced in the framework of a muffin-tin multiple scattering approach by using large clusters of few hundreds of atoms in which the absorbing atom is always at the center of the cluster. The result is compared to the experimental spectrum for a 147-atom cluster ($Pt_{147}$) in Figure 1, showing an overall agreement concerning both the white line and the other structures.

However, the intensity of the line is not the same for a surface atom, which has to be taken into account in particular if one considers smaller clusters, such as $Pt_{13}$ (see Figure 2). Moreover, in the latter case, the edge is shifted ($E = 11\,560$ eV), which is better reproduced by using the new version of the FEFF code (FEFF7) than the previous one (FEFF6). Therefore, in the following all the XANES spectra will be calculated using the FEFF7 code.

## 3. Nanometric Platinum Cluster

In the following, we will consider clusters of increasing size built on an FCC lattice by adding to a central atom (labeled

* To whom correspondence should be addressed.
† Université Paris-Sud.
‡ North Carolina State University.
§ Washington University.
|| CRMC².
⊗ Abstract published in *Advance ACS Abstracts,* June 15, 1997.

S1089-5647(96)03949-1 CCC: $14.00 

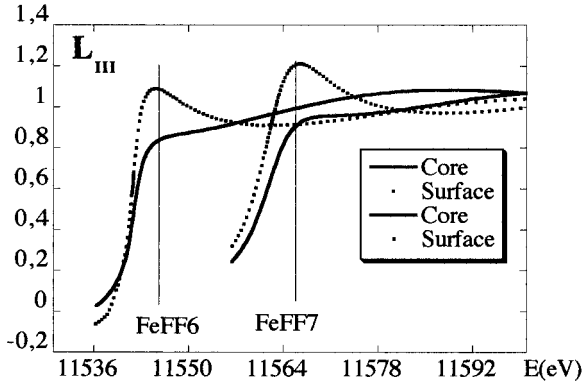


**Figure 2.** XANES of a platinum cluster containing 13 atoms as calculated by FeFF6 and FeFF7 for the central (line) and surface (dots) atoms.

**Figure 3.** Schematic representation of a 13 Pt atom cluster.

$S_0$), the successive shells of its first ($S_1$), second ($S_2$), and third ($S_3$) neighbors, and finally the first neighbors of the first shell ($S_4$). We thus obtains clusters of 13, 19, 43, and 55 atoms.[36−39]

**3.1 The Case of a 13 Platinum Atom Cluster.** Let us first consider the smallest cluster of 13 atoms and try to define the different key parameters for the calculation of the white line. Obviously, when the calculation is done for the central atom, all the surface atoms are equivalent so that they all undergo the same potential. The situation is more complicated for a surface atom of the $S_1$ type (dark grey sphere in Figure 3), since it presents five first neighbors (four equivalent $S_1$, which are light grey in Figure 3, and the center atom $S_0$, which is not visible) and seven more distant ones (all of type $S_1$, which are black in Figure 3). Therefore, at least 3 configurations exist, depending on whether we ascribe the same potential to the 12 neighbors (config. 1) or two different ones for the 4 first neighbors of type $S_1$ and either the same for the 8 others (config. 2) or a different one for the first neighbor of type $S_0$ (config. 3).

The corresponding absorption edges ($\mu$) are plotted and compared to their atomic counterpart ($\mu_0$) for the central atom (Figure 4 for the $L_{II}$ edge and Figure 5 for the $L_{III}$ edge) and the surface atom (Figure 6 for the $L_{II}$ edge and Figure 7 for the $L_{III}$ edge). The most interesting results are those obtained for the surface atom for which the intensity of the white line clearly depends on the choice of the configuration. Surprisingly however, results obtained with configs. 1 and 3 are almost indiscernible (and thus results associated with the config. 3 have not be plotted), even though they significantly differ from those obtained with config. 2.

It can be useful to look at the different physical parameters entering the calculation, namely, the chemical potential Ω, the wavenumber at the Fermi energy $k_f$, the interstitial potential $V_{int}$, and the associated radius $R_{s-int}$. This is done in Table 1 which

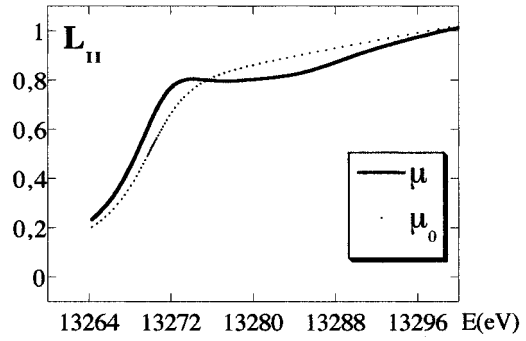


**Figure 4.** White line at the $L_{II}$ edge as calculated by FeFF7 for the central atom.

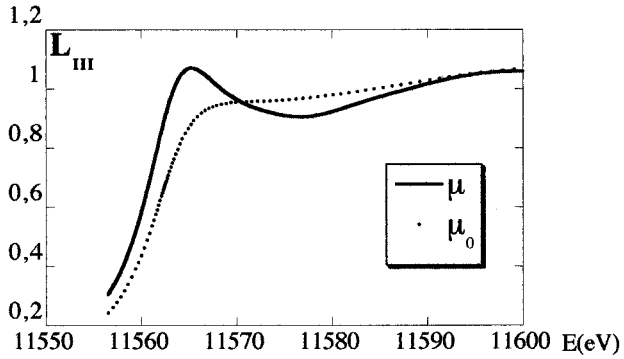


**Figure 5.** White line at the $L_{III}$ edge as calculated by FeFF7 for the central atom.

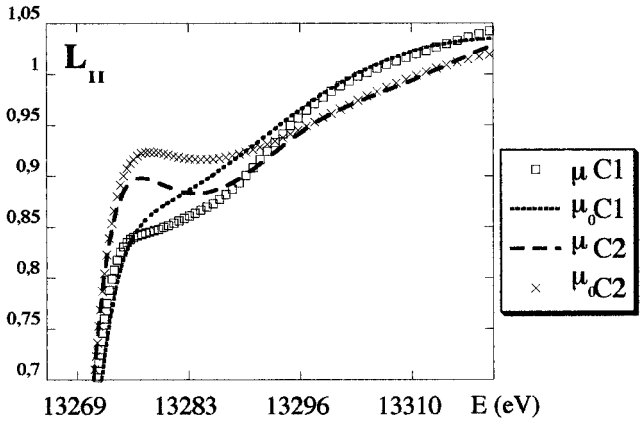


**Figure 6.** $L_{II}$ edge as calculated by FeFF7 for the surface atom for the different configurations: C1 (config. 1), C2 (config. 2).

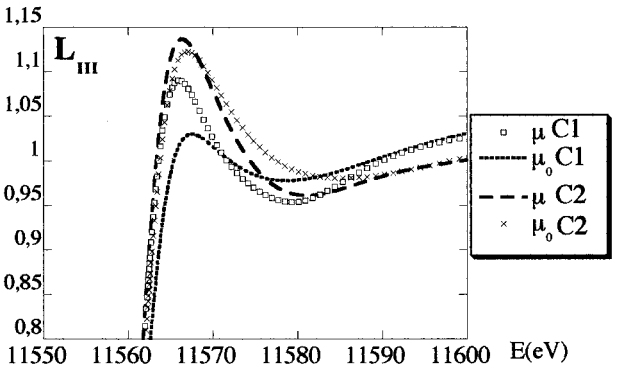


**Figure 7.** $L_{III}$ edge as calculated by FeFF7 for the surface atom for the different configurations: C1 (config. 1), C2 (config. 2).

clearly reveals a correlation between the intensity of the white line and the value obtained for the chemical potential (Ω).

Finally, the quantitative technique for the determination of the number of unoccupied d-electron final states as defined by

**TABLE 1: The Different Physical Parameters Entering the Calculation**

| | config. 1 | config. 2 | config. 3 |
|---|---|---|---|
| chemical potential Ω | −2.78 | −2.63 | −2.76 |
| Fermi energy $k_f$ | 1.662 | 1.80 | 1.67 |
| interstitial potential $V_{int}$ | −1.33 | −1.50 | −1.35 |
| associated radius $R_{s-int}$ | 2.183 | 2.00 | 2.16 |

**TABLE 2: Absolute Areas of the $L_{II,III}$ Edges**

| | config. 1 | config. 2 | config. 3 |
|---|---|---|---|
| $L_{II}$ edge | −0.003 | 0.001 | −0.005 |
| $L_{III}$ edge | 0.0055 | 0.016 | 0.002 |

**TABLE 3: Coordination of Different Types of Atoms inside the Clusters Considered in This Work**

| | $S_0$ | $S_1$ | $S_2$ | $S_3$ | $S_4$ |
|---|---|---|---|---|---|
| $Pt_{13}$ | 12 | 5 | | | |
| $Pt_{19}$ | 12 | 7 | 4 | | |
| $Pt_{43}$ | 12 | 11 | 8 | 5 | |
| $Pt_{55}$ | 12 | 12 | 8 | 7 | 5 |

Mansour et al.[14] is based on a difference between the white line at the $L_{II,III}$ edges of the catalyst and the corresponding feature associated to a reference compound. This differential approach is the crucial point of this method since the difference between the areas can be determined much more accurately than the absolute areas. As we will see through calculations of the density of state, the choice of a reference compound is not so easy in the case of nanometer scale metallic clusters. Nevertheless, this approach has the advantage to give an idea of the magnitude of the effect.

The absolute areas have been calculated between 11 555 and 11 605 eV for the $L_{III}$ and between 13 265 and 13 315 eV for the $L_{II}$ following.[14] Finally, the difference as reported in Table 2 between the area associated with the central atom and the surface atom have been normalized with the value obtained for the central atom. As we can see, due to the integration limits, the difference between all these values is less different than the differences pointed out between the maximum of the white intensities as shown in Figure 2.

**3.2 Size Effect.** We have then repeated the calculation for the series of small platinum clusters previously described. Let us recall that each cluster presents a different number of inequivalent sites, which are defined as sites with different coordination numbers and are detailed in Table 3. For each cluster, we have then calculated the white line corresponding to each inequivalent type of atom (2 for $Pt_{13}$, 3 for $Pt_{19}$, ...).

As already seen in Figure 2 for the $Pt_{13}$ cluster, some variation of the electronic structure at the Fermi level is clearly evidenced between the surface and the core of the cluster: the intensity of the white line is lower for the atom at the center of the cluster ($S_0$) than for the surface atom ($S_1$). The extension of the argument to larger clusters should mean that the various inequivalent sites should give rise to new lines, which should be ordered as $S_0$, $S_1$, $S_2$, $S_3$, $S_4$, ... as a function of increasing intensity of the white line. As can be seen in Figure 8, this is not observed for the $Pt_{19}$ cluster.

This is in fact true for Pt43 (Figure 9) but not for $Pt_{55}$ (Figure 10), for which the white line associated with $S_4$ atoms has not the most important intensity. As a conclusion, though we observe a significant effect of the white line intensity concerning the surface atoms relative to the core ones for all the considered cluster sizes, the variation of this intensity on the different surface sites is more difficult to interpret.

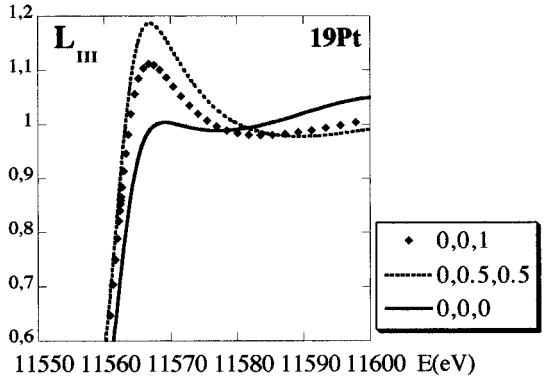


**Figure 8.** Different white lines as calculated by the FeFF7 code for a cluster of 19 atoms of platinum for S0 (line), S1 (dashes), and S2 (diamonds).

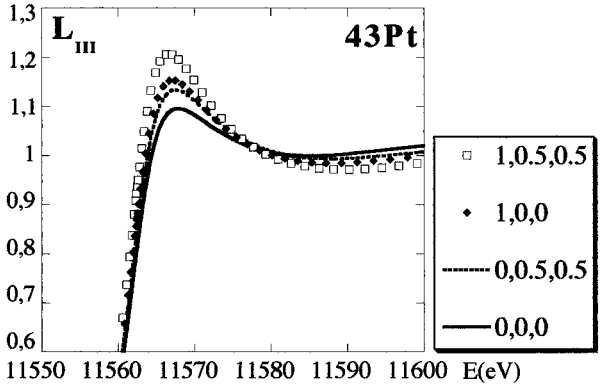


**Figure 9.** Different white lines as calculated by the FeFF7 code for a cluster of 43 atoms of platinum for S0 (line), S1 (dashes), S2 (diamonds), and S3 (squares).

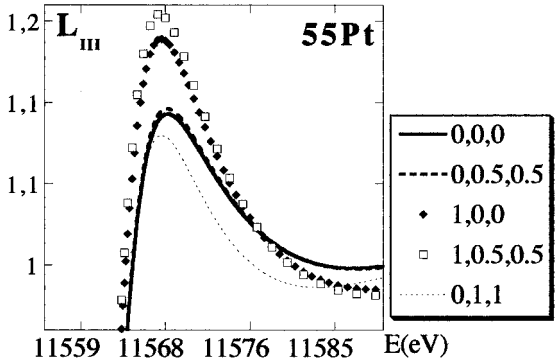


**Figure 10.** Different white lines as calculated by the FeFF7 code for a cluster of 55 atoms of platinum for S0 (line), S1 (dashes), S2 (diamonds), S3 (squares), and S4 (dots).

## 4. Calculation of the Densities of States

A first attempt to characterize this correlation is to relate the variation of the intensity of the white line to the variation of the local density of d states on each inequivalent type of atom. Indeed, the effective width of the local density of states decreases with the coordination number of the site under consideration. As can be derived from the environments previously given in Table 3, one could then conclude that the intensity of the white line given by the FEFF7 calculations increases when the coordination number increases. To go beyond this qualitative argument, the only way is to calculate the electronic densities of states for the various inequivalent sites of small platinum clusters. This is illustrated in Figure 11, where we plot the local densities of state (LDOS) of low-coordinated surface sites of a large Pt cuboctahedron (3871 atoms).

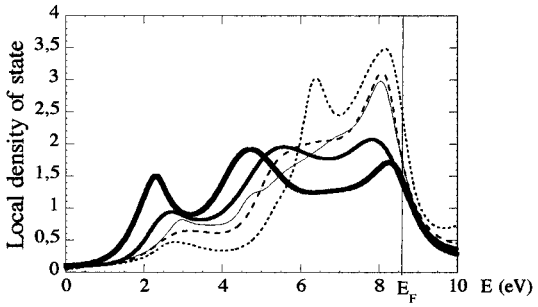


**Figure 11.** Local densities of states at the 3871 Pt cuboctahedron surface for the vertex (•••), the edge (---), the (100) (thin line) and (111) (thick line) facets, and the central atom (very thick line).

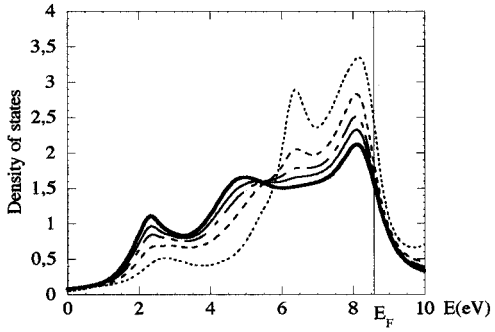


**Figure 12.** Averaged densities of states of 13 atom (•••), 55 atom (---), 147 atom (−•−), 309 atoms (thin line), and 923 atom (thick line) Pt cuboctahedra.

The calculations are performed in a tight-binding model including spd-hybridization which is detailed elsewhere[40] except for the charge neutrality rule. Indeed, instead of the assumption of global neutrality used in ref 40, we proceed via a partial neutrality by orbital according to recent *ab initio* calculations performed on transition metal surfaces.[41] The self-consistency treatment implies then to shift each orbital level (independently for s, p, and d orbitals in order to keep the neutrality by orbital) depending on the site coordination.

Such a procedure could be questionable for small size clusters. A previous experimental and theoretical study of correlation effects in clusters of Ni and Pd as a function of their size[42] showed that whereas the width of the UPS spectra increases for both metals when the size increases, the width of their Auger spectra increases for palladium and decreases for nickel. This was theoretically interpreted as due to a possible change in electronic configuration between the atom and the solid, modifying their Auger line width via electronic correlation effects. However, according to the *ab initio* calculations already mentioned,[41] the assumption of global neutrality requires keeping the electronic configuration of the solid for sufficiently large clusters (many tens of atoms). For smaller sizes, it would be interesting to perform new *ab initio* calculations on Pt clusters (which has never be done to our knowledge) in order to describe their electronic structure and in particular the link between the atomic and solid electronic configurations. Thus, we obtain specific local densities which differ by their bandwidth and their values near the Fermi level, even though their number of electrons remains constant independent of the site and of the cluster size.

The densities of states (DOS) for different cluster sizes are presented in Figure 12. They are obtained by averaging the local densities of states on all the inequivalent sites (vertex; $S_N$; edge, $S_{N-1}$; facets, $S_{N-2}$, $S_{N-3}$; "core", $S_{N-4} = ... = S_0$) present in the cluster depending on the size. That explains why the $Pt_{13}$ cluster density is quite the same as the local density of a vertex whereas when the size increases, the averaged density tends to the bulk one.

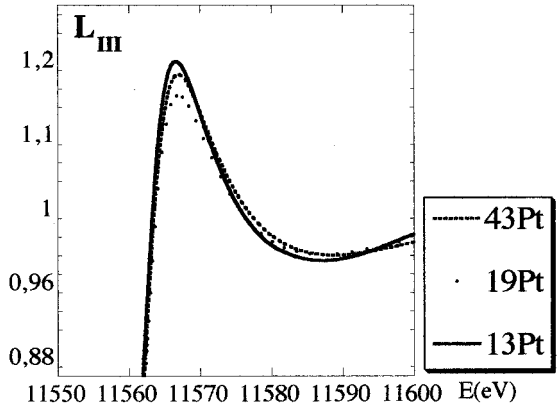


**Figure 13.** Size effect on the Xanes spectrum for $Pt_{13}$ (line), $Pt_{19}$ (dots), and $Pt_{43}$ (dashes).

Let us try now to relate the intensity of the white line to the size of the cluster. To this aim, we calculate the XANES spectra of nanometer metallic particles by averaging the contribution of each type of atom. As shown in Figure 13, the intensity of the white line varies slowly with the size of the cluster. This is a direct consequence of the existence of inequivalent sites in small clusters, which means that a size effect is directly observable on the white line. Thus, at least two physical phenomenon can affect the intensity of the white line: the size of the cluster, which can be considered as an intrinsic effect, and a charge transfer between the cluster and the support, which can be considered as an extrinsic one. Finally, this size cluster effect as calculated by the FeFF7 program seems to be small and thus it may be difficult to determine the cluster size on the basis of the magnitude of the white line.

Despite these advances in our theoretical understanding of the X-ray absorption white lines, numerical simulations regarding either the $L_{II,III}$ edges or the density of state and experimental measurements cannot yet be directly compared. The main reason is due to the fact that the interaction between the platinum cluster and the support is not taken into account. Here, we can assume that a major improvement in the theoretical calculations can be done through a comparison between the density of state calculated by the FeFF program and the one based on a tight-binding model. This approach will allow us to properly handle electronic transfer between the cluster and the support or between the two metals inside the particle.

## 5. Conclusion

Through all the calculations dedicated to the electronic structure of nanometer scale clusters as well as the $L_{II,III}$ edge of platinum, we have shown that a strong correlation exists between the intensity of the white line and the size of the cluster. Thus, at least two physical phenomenon can affect the intensity of the white line: the size of the cluster which can be considered as an intrinsic effect (density of state of nanometer scale platinum cluster is far from the bulk one), and a possible charge transfer between the cluster and the support, which can be considered as an extrinsic one. Thus through a comparison between the white line of the platinum-based catalyst and the white line of a platinum foil, we show that assuming charge transfer is not necessary to explain the variations of the white line intensity.

Also, if the first results obtained with the FeFF program are encouraging, it is clear that to go further in the analysis, the detailed geometric configurations present in the cluster surface

have to be integrated very precisely in order to obtain quantitative effects which would be more clearly related to the characteristics of the density of states.

## References and Notes

(1) Cauchois, Y.; Mott, N. F.; *Philos. Mag.* **1949**, *40*, 1260.
(2) Lytle, F. W.; Sayers, D. E.; Stern, E. A. *Phys. Rev. B* **1975**, *15* (4), 2426.
(3) Tamura, E.; Van Ek, J.; Froba, M.; Wong, J. *Phys. Rev. Lett.* **1995**, 74−24, 4899.
(4) Boyun, Qi; Perez, I.; Ansari, P. H.; Lu; F.; Croft, M. *Phys. Rev. B* **1995**, *36* (5), 2972.
(5) Brown, M.; Peierls, R. E.; Stern, E. A. *Phys. Rev. B* **1994**, *15* (2), 738.
(6) Parthasaradhi, K.; Esposito, A.; Mobilio, S.; Pelliccioni, M. *Phys. Rev. A* **1995**, *38* (3), 1608.
(7) Fujikawa, T.; Matsuura, T.; Kuroda, H. *J. Phys. Soc. Jpn.* **1983**, *52* (3), 905.
(8) Matsuura, T.; Fujikawa, T.; Kurodda, H. *J. Phys. Soc. Jpn.* **1983**, 52 (9),3275.
(9) Biebesheimer, V. A.; Marques, E. C.; Sandstrom, D. R.; Lytle, F. W.; Greegor, R. B. *J. Chem. Phys.* **1984**, *81* (6), 2599.
(10) Lytle, F. W. *J. Catal.* **1976**, *43*, 376.
(11) Lytle, F. W.; Wei, P. S. P.; Greegor, R. B.; Via, G. H.; Sinfelt, J. H. *J. Chem. Phys.* **1979**, *70* (11), 4849.
(12) Ichikuni, N.; Iwasawa, Y. *Catal. Lett.* **1993**, *20*, 87.
(13) Mansour, A. N.; Cook, J. W.; Sayers, D. E. *J. Phys. Chem.* **1984**, *88*, 2330.
(14) Mansour, A. N.; Sayers, D. E.; Cook, J. W.; Short, D. R.; Shannon, R. D.; Katzer, J. R. *J. Phys. Chem.* **1984**, *88*, 1778.
(15) Richard, D.; Couves, J. W.; Thomas, J. M. *Faraday Discuss.* **1991**, *92*, 109.
(16) Hill, E. K.; Baudoing-Savois, R.; Moraweck, B.; Renouprez, A. J. *J. Phys. Chem.* **1996**, *100*, 3102.
(17) Bazin, D.; Dexpert, H.; Lynch, J. In *X-ray Absorption Fine Structure for catalysts and surfaces*; Iwasawa, Y., Ed.; World Scientific: London 1996.
(18) Bazin, D.; Dexpert, H.; Lagarde, P.; Bournonville, J. P. *J. Catal.* **1988**, *110*, 209.
(19) Bazin, D.; Dexpert, H.; Bournonville, J. P.; Lynch, J. *J. Catal.* **1990**, *123*, 86.
(20) Fernandez-Garcia, M.; Marquez Alvarez, C.; Haller, G. L. *J. Phys. Chem.* **1995**, *99*, 12565.
(21) Bazin, D.; Sayers, D. *Jpn. J. Appl. Phys.* **1993**, *32* (2), 249.
(22) Bazin, D.; Sayers, D. *Jpn. J. Appl. Phys.* **1993**, *32* (2), 252.
(23) Samant, M. G.; Bergeret, G.; Meitzner, G.; Gallezot, P.; Boudart M. *J. Phys. Chem.* **1988**, *92*, 3542.
(24) Samant, M. G.; Bergeret, G.; Meitzner, G.; Gallezot, P.; Boudart, M. *J. Phys. Chem.* **1988**, *92*, 3547.
(25) Bergeret, G.; Gallezot, P. In *Determination of the atomic structure of solid catalysts by X-ray diffraction*; Dunod, Ed.; Montrouge Cedex, France, 1993.
(26) Clausen, B. S.; Grabaek, L.; Steffensen, G.; Hansen, P. L.; Topsoe, H. *Catal. Lett.* **1993**, *20*, 23.
(27) Thomas, J. M.; Greaves, G. N.; Catlow, C. R. A. *Nucl. Instrum. Methods* **1995**, *397*, 1.
(28) Rehr, J. J.; Albers, R. C. *Phys. Rev. B* **1990**, *41*, 8149.
(29) Mustre De Leon, J.; Rehr, J. J.; Zabinski, S. I.; Albers, R. C. *Phys. Rev. B* **1991**, *44* (9), 4146.
(30) Rehr, J. J.; Albers, R. C.; Zabinski, S. I. *Phys. Rev. Lett.* **1992**, *69* (23), 3397.
(31) Natoli, C. R.; Misemer, D. K.; Doniach, S.; Kutzler, F. W. *Phys. Rev. A* **1980**, *22*, 1104.
(32) Greaves, G. N.; Durham, P. J.; Diakun, G.; Quinn, P. *Nature* **1981**, *294*, 139.
(33) Bazin, D.; Bensaddik, A.; Briois, V.; Sainctavit, Ph; *J. Phys.* **1996**, *C4* (6), 481.
(34) Zabinsky, S. I.; Rehr, J. J.; Ankudinov, A.; Albers, R. C.; Eller, M. J. *Phys. Rev. B* **1995**, *52* (4), 2995.
(35) Zabinsky, S. I. Ph.D. Thesis, University of Washington, 1995.
(36) Mackay, A. *Acta Crystallogr.* **1962**, *15*, 916.
(37) Gordon, M. Thesis, Université of Grenoble, 1978.
(38) Raoult, B.; Farges, J.; De Feraudy, M. F.; Torchet, G. *Philos. Mag.* **1989**, *60*, 881.
(39) Khoutami, A. Thesis, Université d'Orsay, 1993.
(40) Legrand, B.; Treglia, G.; Ducastelle, F. *Phys. Rev. B* **1990**, *41* (7), 4422.
(41) Sawaya, S.; Goniakowski, J.; Treglia, G.; Mottet, C.; Saul A., to be published.
(42) Bellamy, B.; Masson, A.; Degouveia, V.; Desjonqueres, M. C.; Spanjaard, D.; Treglia, G. *J. Phys.: Condens. Matter*, **1989**, *1*, 5875.